Development 135, 1169-1178 (2008) doi:10.1242/dev.014142

Alternative promoter use in eye development: the complex role and regulation of the transcription factor MITF

Kapil Bharti, Wenfang Liu, Tamas Csermely*, Stefano Bertuzzi and Heinz Arnheiter†

During vertebrate eye development, the transcription factor MITF plays central roles in neuroepithelial domain specification and differentiation of the retinal pigment epithelium. MITF is not a single protein but represents a family of isoforms generated from a common gene by alternative promoter/exon use. To address the question of the role and regulation of these isoforms, we first determined their expression patterns in developing mouse eyes and analyzed the role of some of them in genetic models. We found that two isoforms, A- and J-Mitf, are present throughout development in both retina and pigment epithelium, whereas H-Mitf is detected preferentially and D-Mitf exclusively in the pigment epithelium. We further found that a genomic deletion encompassing the promoter/exon regions of H-, D- and B-Mitf leads to novel mRNA isoforms and proteins translated from internal start sites. These novel proteins lack the normal, isoform-specific N-terminal sequences and are unable to support the development of the pigment epithelium, but are capable of inducing pigmentation in the ciliary margin and the iris. Moreover, in mutants of the retinal *Mitf* regulator *Chx10* (*Vsx2*), reduced cell proliferation and abnormal pigmentation of the retina are associated with a preferential upregulation of H- and D-Mitf. This retinal phenotype is corrected when H- and D-Mitf are missing in double *Mitf*/*Chx10* mutants. The results suggest that *Mitf* regulation in the developing eye is isoform-selective, both temporally and spatially, and that some isoforms, including H- and D-Mitf, are more crucial than others in effecting normal retina and pigment epithelium development.

KEY WORDS: Retina, Retinal pigment epithelium, *Mitf red-eyed white*, *Mitf black-eyed white*, *Chx10-ocular retardation*, Internal start codons

INTRODUCTION

Alternative promoter use is a common principle by which genes generate transcript diversity and contribute to an organism's phenotypic complexity. Often, promoter choice does not affect the sequence of the corresponding proteins because translation is invariably initiated from a single downstream start site, but the untranslated 5′ regions can influence mRNA stability and translational efficiency and so refine gene regulation beyond the spatial and temporal control afforded at the transcriptional level. With some genes, however, variant 5′ exons encode unique amino acid sequences and hence provide an additional level of regulation as protein isoforms with distinct N-termini can differ in their function (Carninci et al., 2006; Sandelin et al., 2007). Nevertheless, despite a wealth of sequence information for many species, relatively little is known about the role and regulation of alternative promoter use in vivo, both during development and in adulthood.

A prime example of a gene with multiple promoters is *Mitf* (microphthalmia-associated transcription factor), which encodes a basic helix-loop-helix leucine-zipper protein that is crucial for mammalian eye development (Hodgkinson et al., 1993; Nakayama et al., 1998; Nguyen and Arnheiter, 2000). In mice and humans, the gene contains nine distinct promoters, six of which are linked to different coding exons and three to non-coding exons (Fig. 1) (Hallsson et al., 2000; Steingrimsson et al., 2004; Hershey and Fisher, 2005; Arnheiter et al., 2006; Hallsson et al., 2007). Using probes that do not distinguish between the corresponding isoforms, it has been shown that *Mitf* is initially expressed in mice throughout the budding optic vesicle and retained in the future retinal pigment epithelium (RPE), the ciliary body and the iris, but is downregulated in the future retina and optic stalk (Bora et al., 1998; Nguyen and Arnheiter, 2000). In *Mitf* mutants in which all isoforms are equally affected, the RPE can develop as a laminated second retina (Müller, 1950; Bumsted and Barnstable, 2000; Nguyen and Arnheiter, 2000), and in mutants in which *Mitf* is abnormally upregulated in the retina, the retina can develop as a single-layered RPE (Rowan et al., 2004; Horsford et al., 2005; Bharti et al., 2006). From these results, however, it remains unclear which isoforms are normally expressed during RPE and retina formation and whether any of these isoforms have selective roles or are entirely interchangeable.

The question of isoform-specific function and expression also touches on the problem of whether distinct isoforms are co-regulated or regulated separately. In fact, two lines of evidence argue in favor of co-regulation. One is the observation, made in mice, that the combined genetic lack of the eye transcription factors PAX2 and PAX6 is associated with a total absence of all MITF protein. This finding is supported by the notion that the human A-MITF promoter, which, like the mouse A-Mitf promoter, is located at the 5′ end of the gene, is stimulated by PAX2/PAX6 in vitro, and hence might serve as a control region for the entire *MITF* locus in the eye in vivo (Bäumer et al., 2003). The other is the recent observation that the paired-like homeodomain transcription factor CHX10 (also known as VSX2 – Mouse Genome Informatics), which is involved in the retinal downregulation of *Mitf* (Liu et al., 1994; Burmeister et al., 1996; Rowan et al., 2004; Horsford et al., 2005), may stimulate a cluster of genes encoding microRNAs that serve to suppress *Mitf* mRNAs by recognizing their common 3′UTRs (Xu et al., 2007). Without more-detailed information about the developmental expression pattern of each *Mitf* isoform, however, an isoform-selective regulation cannot be excluded a priori.

Mammalian Development Section, National Institute of Neurological Disorders and Stroke, National Institutes of Health, Bethesda, MD 20892, USA.

*Present address: Department of Anaesthesiology, Hospital of Hungarian Defense Forces, Robert K. 44, 1134, Budapest, Hungary
†Author for correspondence (e-mail: ha3p@nih.gov)

Accepted 7 January 2008

Here, we use a combination of tissue dissection, reverse transcriptase-PCR and isoform-specific antibodies to show that some *Mitf* isoforms are ubiquitously expressed throughout development in both ocular and extraocular tissues, that others are more restricted to the optic neuroepithelium, and others still are retained exclusively in the RPE. We then analyze two different mouse mutations associated with over- or underexpression of *Mitf* to assess the functional relevance of some of these isoforms in both retina and RPE. The results indicate that contrary to previous assumptions, the regulation of *Mitf* during eye development is not simply global, affecting all transcriptional isoforms indiscriminately, but in fact is isoform-selective. They also suggest that some isoforms are more crucial than others for early cell-fate decisions in the developing eye, and hence for the formation of a functional adult eye.

MATERIALS AND METHODS

Animals

C57BL/6J control mice were from Jackson Laboratories (Bar Harbor, ME) and albino Swiss Webster (SW-*Tyr*^{c}) mice were from Taconic (Rockville, MD). The following mutant mice were bred locally and kept according to NINDS-approved animal study proposals: C57BL/6J-*Mitf*$^{mi\text{-}rw}$, mixed (C57BL/6J;C3H/HeJ)-*Mitf*$^{mi\text{-}bw}$, C57BL/6J•C3H/HeJ-*Mitf*$^{mi\text{-}vga9}$, used as N7F2, and C57BL/6J•129S1/Sv-*Chx10*^{orJ}, used as N10F12-F16.

Antibodies, immunohistochemistry, immunofluorescence and in situ hybridization

Pan-specific rabbit antibodies against MITF have been described (Nakayama et al., 1998). An MITF exon 1B1b-specific antibody was prepared by immunizing rabbits with a synthetic peptide (SRILLRQQLMREQMQEQERR) and affinity purifying the resulting serum using a corresponding peptide column. A mouse monoclonal antibody to the C-terminus of MITF was prepared by standard procedures after immunizing mice with a recombinant mouse MITF fragment corresponding to residues 298-419 (exon 9) tagged with GST. Clone 6A5 (IgG1, κ) was used as ascites fluid made from ICR SCID mice. A rabbit anti-mouse-tyrosinase serum was a gift from Dr Vincent Hearing (National Cancer Institute, National Institutes of Health, Bethesda, MD). The following antibodies were obtained from commercial sources: rabbit anti-PAX6 and mouse monoclonal anti-TUJ1 (Covance Research); rabbit anti-cyclin D1 and rabbit anti-phosphohistone (Upstate Biotechnology); mouse monoclonal against V5 tag (Invitrogen); sheep anti-N-terminus of CHX10 (Abcam); sheep anti-C-terminus of CHX10 (Exalpha Biologicals).

Immunolabeling was performed on 14-μm cryostat sections as described previously (Nakayama et al., 1998), except for the exon-specific anti-1B1b antibody, which required antigen retrieval by boiling the sections for 30 minutes.

In situ hybridization was performed using a pan-specific *Mitf* probe as described (Nakayama et al., 1998), or a PCR-generated exon 1B1b-specific probe (primer sequences available upon request).

Reverse transcription (RT) reactions and real-time PCR

RNA was isolated by two means. (1) RNA extractions using the RNeasy Mini Kit (Qiagen). E9.5 and 10.5 eye primordia were manually dissected along with the surrounding tissue. E11.5-P0 retinal tissue was separated manually from the surrounding RPE/mesenchyme, except where indicated. cDNA was prepared using the Superscript RT-PCR Kit (Invitrogen), using 1 μg of total RNA, and cDNA corresponding to 25 ng of total template RNA was used for each PCR reaction. (2) RNA was isolated using the Picopure RNA Extraction Kit (Arcturus) from 100 cells that were microscopically selected after trypsinization, using micromanipulator-controlled glass microinjection pipettes. In these cases, the amount of cDNA used for amplification with two rounds of PCR using nested primer pairs was estimated to correspond to approximately 1-10 pg of template RNA.

Real-time PCR was performed using an ABI Prism 7000 real-time PCR machine (Applied Biosystems). All RT-PCR products were sequenced at least once to confirm primer specificity. In the eye, sequencing provided no evidence for alternative splicing events linking exon 1A with exon 1J1b, nor exon 1J1b with exon 1C1b, as reported for cultured cell lines (Hershey and Fisher, 2005). Therefore, exons 1J and 1C are here considered as single exons. Primer sets used for RT-PCR and real-time PCR are available upon request.

For Fig. 3B, eyes from 20 E11.5 and 12 E15.5 wild-type embryos were manually dissected to give separate RPE/mesenchymal and retinal fractions. RNA was isolated using the RNeasy Mini Kit. The following procedure was used to generate standard curves and assay the test samples (Fig. 3B). First, isoform-specific cDNAs were generated by PCR using isoform-specific forward primers and a common reverse primer in exon 1B1b. Second, the cDNAs were quantitated spectrophotometrically and quantitation was confirmed by agarose gel electrophoresis. To generate standard curves, appropriate concentrations of the quantitated cDNAs were diluted into cDNA prepared from hearts of *Mitf*$^{mi\text{-}rw/mi\text{-}rw}$ animals. The *rw* cDNA lacks exon 1B corresponding to the common reverse primer but mimics the cDNA complexity of the test samples, thereby providing an amplification environment for the standards that is similar to that provided by the test samples. Real-time PCR of the cDNA standards was performed with exon-specific forward primers and a common reverse primer in exon 1B1b. Standard curves were generated for each isoform, and separately for each repeat assay performed with the test sample. Real-time PCR of the test samples was performed (four independent assays, each in triplicate), using appropriate primers. Absolute amounts of cDNAs were determined using the appropriate isoform-specific standard curves. The calculated amounts represent the levels of the respective isoforms in cDNA prepared from 25 ng of total RNA and confirmed as giving equal amplification of *Gapdh* and β-actin cDNAs. Considering that mRNAs represent approximately 3% of total RNA, and RT efficiency is approximately 10%, the isoform-specific levels shown in Fig. 3B correspond to approximately 75 pg of mRNA.

For Fig. 4, 14 whole eyes each from E12.5 wild-type and *Mitf*$^{mi\text{-}rw/mi\text{-}rw}$ embryos, and from P0 wild-type and *Mitf*$^{mi\text{-}rw/mi\text{-}rw}$ mice were used. RNA isolation, RT reactions, and real-time PCR were as above except that: (1) single-exon-specific primers were used; (2) the measurements were repeated three times, each time in triplicate; and (3) the results are given as the ratio between the amounts measured in *Mitf*$^{mi\text{-}rw/mi\text{-}rw}$ and in wild-type cDNAs. This means that unlike for Fig. 3B, there was no need for isoform-specific standard curves. However, to correct for variations between samples, wild-type and mutant results were first normalized to the internal β-actin and *Gapdh* levels.

Molecular characterization of the *Mitf*$^{mi\text{-}rw}$ mutation, constructs, in vitro mutagenesis and reporter assays

The *Mitf*$^{mi\text{-}rw}$ mutation was characterized by PCR and Southern blots (see Fig. S1 in the supplementary material). The various *Mitf* isoforms were cloned and their activities assayed in vitro (see Fig. S2 in the supplementary material).

Chromatin immunoprecipitation (ChIP) assays

For details of ChIP assays using anti-CHX10 antibodies and amplification of *Mitf* promoter DNA see Figs S3, S4 in the supplementary material. Primer sequences are available upon request.

RESULTS

Mitf mRNA and protein expression in the developing mouse eye

Previous studies using pan-specific in situ hybridization probes and antibodies have shown that *Mitf* expression in the developing eye begins at around embryonic day (E) 9.5 and lasts until postnatal day (P) 0 (Nakayama et al., 1998; Nguyen and Arnheiter, 2000). To analyze the isoform composition of this pan-specific signal, we first used an in situ hybridization probe specific for exon 1B1b, which is common to all isoforms except M-Mitf (Fig. 1), a major component of neural crest-derived choroidal and iris melanocytes. As shown in Fig. 2A, exon 1B1b is expressed in the optic vesicle at E9.5, is downregulated in the distal optic vesicle at E10.0, and is then concentrated in the developing RPE as previously reported for a

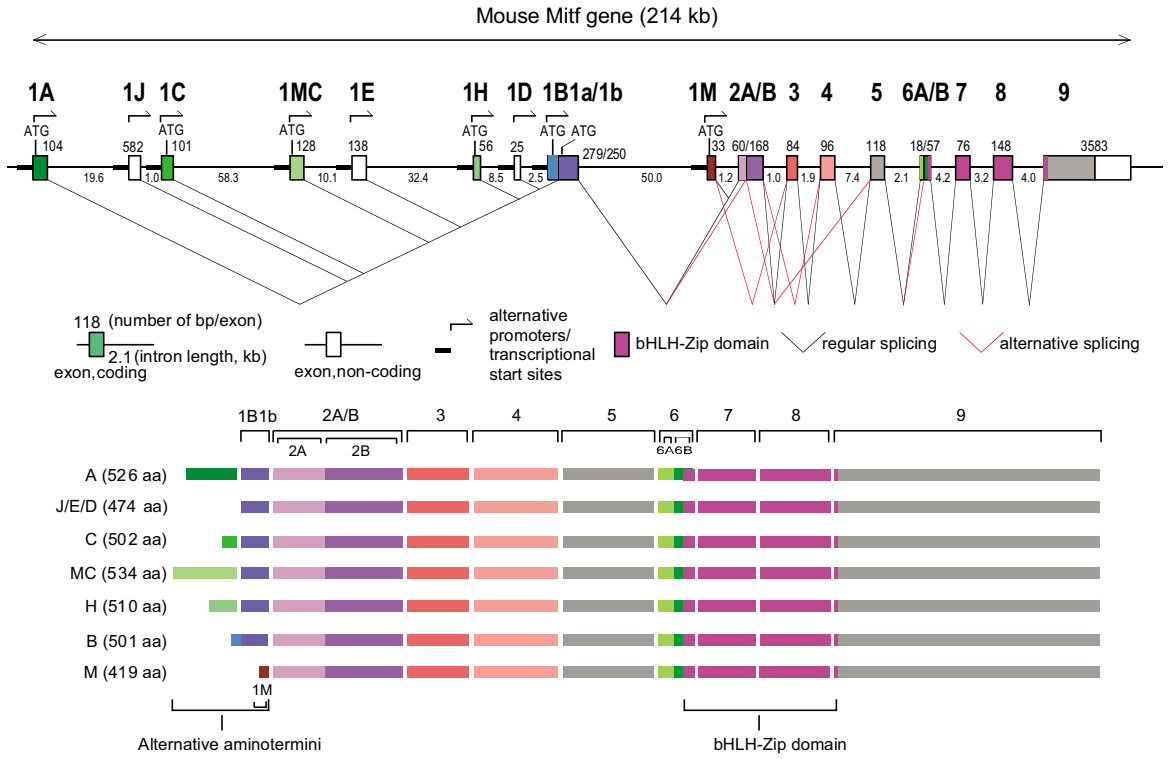

Fig. 1. Generation and structure of MITF isoforms in mouse. (Top) Schematic of the mouse *Mitf* gene with its multiple promoters and regular and alternative splice choices. (Bottom) Schematic of the seven protein isoforms that differ in their N-terminal sequences owing to different promoter choice.

single time point (Amae et al., 1998). As expected, no labeling was seen in choroidal and iris melanocytes, which start to accumulate at around E11.5 on the proximal side of the RPE and normally are labeled with pan-specific probes (Nakayama et al., 1998). Also, no labeling was seen on sections from *Mitf*$^{mi\text{-}rw}$ (*Mitf red-eyed white*) embryos (Fig. 2A, right-most panel), which carry a genomic deletion of exon 1B (Hallsson et al., 2000) but express *Mitf*, as detectable with pan-specific probes (see below, Fig. 5F).

To determine whether exon 1B1b-containing mRNAs are translated into corresponding proteins, we performed a series of immunoblot, immunoprecipitation and immunohistochemical analyses. The specificity of an antibody for exon 1B1b-containing MITF (reactivity with A-, J- and D-MITF, but not M-MITF) is shown in Fig. 2B, along with the pan-specific reactivity of a mouse monoclonal antibody to the MITF C-terminal domain (CTD) and the absence of reactivity of either antibody with normal fibroblast extracts. Using these antibodies, we then performed a combined immunoprecipitation/immunoblot assay of extracts of RPE/choroids and retinas that were manually dissected and separately pooled from approximately 100 eyes of wild-type E12.5 embryos. The results revealed at least three bands in RPE/choroid and one band of lower electrophoretic mobility in retina (Fig. 2B, bottom right panel, arrowheads). This finding indicates that RPE/choroid and retina express distinct exon 1B1b-containing isoforms, but, based on electrophoretic mobility alone, their precise identification is not feasible because post-translational modifications might potentially modify their apparent molecular weights.

In immunohistochemical assays (Fig. 2C), both exon 1B1b- and pan-specific rabbit antibodies gave overlapping expression patterns in the neuroepithelial parts of the developing eye, starting from E9.5, when MITF is expressed in the entire optic vesicle, through E17.5 and beyond (not shown), when it is expressed predominantly in the RPE. Neural crest-derived choroidal melanocytes, however, were only labeled with the pan-specific antibody (arrows in Fig. 2C, panel labeled wt E15.5). Both exon 1B1b- and pan-specific antibodies gave a low-level labeling in the retina and surrounding mesenchyme when compared with equivalently treated sections from *Mitf*$^{mi\text{-}rw/mi\text{-}rw}$ embryos, which lack exon 1B (Hallsson et al., 2000), or with *Mitf*$^{mi\text{-}vga\text{-}9/mi\text{-}vga\text{-}9}$ embryos, which lack MITF entirely (Hodgkinson et al., 1993; Nakayama et al., 1998) (Fig. 2C, panels labeled *Mitf*$^{mi\text{-}rw/mi\text{-}rw}$ or *Mitf*$^{mi\text{-}vga\text{-}9/mi\text{-}vga\text{-}9}$). This result is consistent with the observation presented in Fig. 2B, showing that E12.5 retinas continue to express at least some isoform(s) of MITF.

Expression of promoter-specific *Mitf* isoforms

To determine the expression profile of individual isoforms, we exclusively used RT-PCR, primarily because it provides the sensitivity to detect low-abundance isoforms. For the early time points (E9.5-10.5), RNA was obtained from whole-eye primordia including the surrounding tissue, and for the later time points (E11.5-P0), separately from RPE/choroidal and retinal fractions. cDNAs were amplified using either the respective 5′ exon-specific forward primers in combination with a reverse primer in exon 1B1b, or, in the case of M-Mitf, a reverse primer in exon 2A. Pan-specific primers corresponded to exons 2A and 4. The number of PCR cycles was adapted for each primer pair to give amplification in the linear range. As shown in Fig. 3A, the first signal was seen at E9.5 with pan-specific primers and weakly with A- and J-Mitf-specific primers, whereas H- and D-Mitf-specific amplification gave the first signals at E10.5. No other isoforms were detected at these early stages.

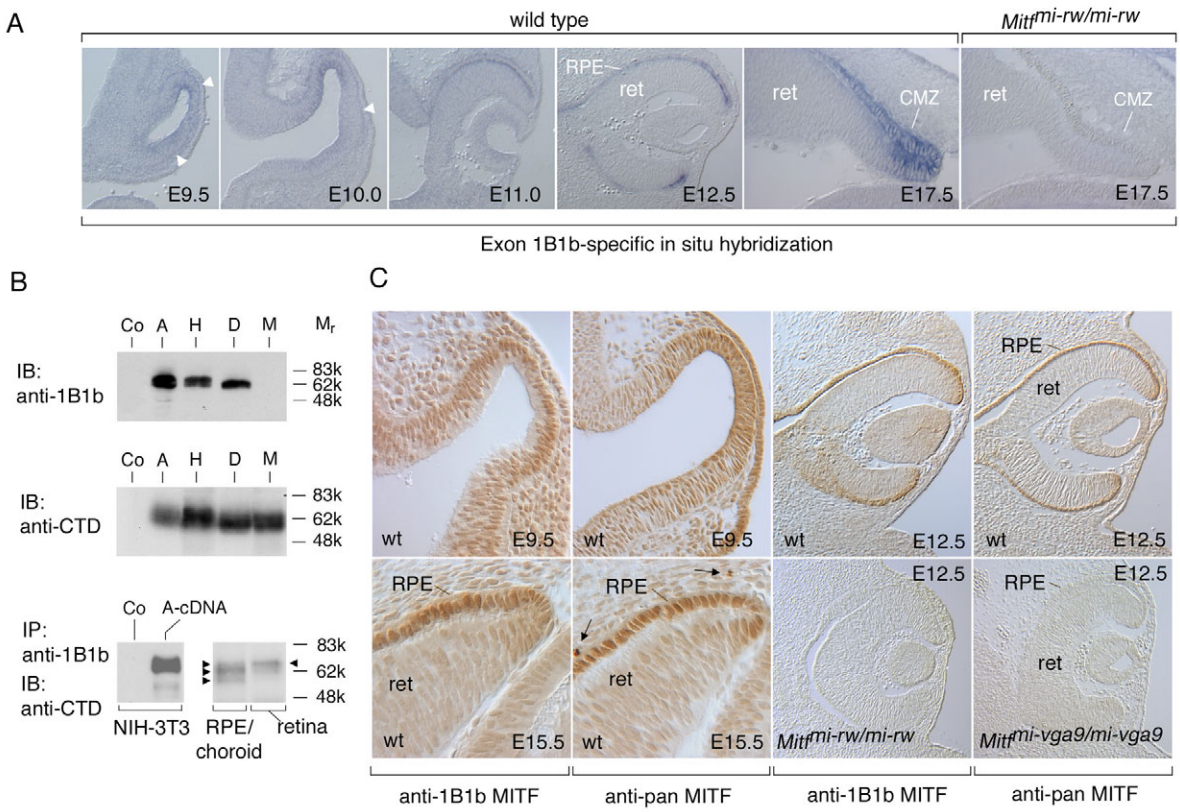

Fig. 2. Expression of *Mitf* RNAs and proteins containing exon 1B1b. (**A**) In situ hybridization with an exon 1B1b-specific probe on frontal sections of the developing mouse eye at the indicated time points. Arrowheads at E9.5 indicate expression of exon 1B1b-containing *Mitf* RNAs throughout the optic vesicle, and the arrowhead at E10.5 indicates reduced expression in the distal optic vesicle. In a control section of an $Mitf^{mi\text{-}rw/mi\text{-}rw}$ embryo, which lacks exon 1B1b, there is no labeling (right-most panel). (**B**) Antibody characterization and *Mitf* expression in RPE/choroid and retina. A-, H-, D-, and M-Mitf cDNAs were expressed in NIH3T3 cells and extracts blotted with polyclonal anti-1B1b MITF antibodies (top panel) or monoclonal anti-MITF C-terminal-domain antibodies (anti-CTD, middle panel). The bottom left panel shows a combined immunoprecipitation (IP)/immunoblot (IB) of NIH-3T3 cells transfected with A-Mitf. The bottom right panel shows a similar IP/IB of extracts from RPE/choroidal and retinal fractions from 100 wild-type eye primordia (E12.5). Arrowheads point to MITF isoforms with distinct electrophoretic mobilities. (**C**) Immunohistochemistry of frontal cryosections of embryos of the indicated genotypes and ages using anti-1B1b MITF and anti-pan-MITF antibodies. Arrows in the panel labeled wt E15.5 point to M-MITF-expressing neural crest-derived melanocytes that are only seen with pan-MITF-specific antibodies. Note that 'wt' refers to Tyr^{c} (albino) embryos carrying a wild-type *Mitf* allele. RPE, retinal pigment epithelium; ret: retina; CMZ, ciliary margin zone.

During the subsequent developmental time points, the different isoforms could be grouped into four distinct expression patterns (Fig. 3A). First, throughout the period from E11.5 to P0, A- and J-Mitf showed similar expression profiles, both in the retina and the RPE/choroid. Second, H-Mitf was preferentially found in the RPE/choroid but was present at low levels in the retina as well, particularly after E15.5. Third, D- and M-Mitf were found only in the RPE/choroid and not the retina. Fourth, C-, MC-, E- and B-Mitf were undetectable, or only barely detectable, throughout development in either retina or RPE/choroid (not shown). In support of these results, from E11.5 to P0, pan-specific amplification showed higher expression levels in RPE/choroid compared with retina. Additional assays indicated that the *Mitf*-related genes *Tfe3*, *Tfeb* and *Tfec* (also known as *Tcfe3*, *Tcfeb* and *Tcfec*, respectively – Mouse Genome Informatics) (Hallsson et al., 2007), were also expressed in the developing eye, and amplification for *Chx10*, which in the eye is retina-specific (Liu et al., 1994), gave a signal only in the retinal fraction. This latter finding, together with the fact that D- and M-Mitf were only seen in the RPE/choroidal fraction, indicates that efficient tissue separation had been achieved.

The above analysis established a temporal expression profile for each isoform, but did not address the question of which isoform is expressed specifically in the RPE because the RPE/choroidal fraction contains other cells, including choroidal melanocytes, that might contribute exon 1B1b-containing isoforms detectable by PCR. Therefore, we repeated the above analysis by specifically selecting retinal, mesenchymal and RPE cells. For these experiments, we used eyes from $Mitf^{mi\text{-}bw}$ (*Mitf black-eyed white*) embryos, whose only pigmented cells are RPE cells as they lack choroidal melanocytes (Yajima et al., 1999). In postnatal eyes of such mice, M-Mitf mRNAs are missing, full-length exon 1B1b-containing mRNAs are reduced, and skipping of common downstream exons is increased (Yajima et al., 1999). At E11.5 through E17.5, however, we found no differences between $Mitf^{mi\text{-}bw}$ and wild-type eyes in *Mitf* expression, except that M-Mitf was lacking in the mutant (not shown). Hence, the use of separately trypsinized RPE/mesenchymal and retinal fractions of E15.5 $Mitf^{mi\text{-}bw/mi\text{-}bw}$ allowed us to select microscopically small populations (100 cells) of pure mesenchymal, RPE or retinal cells (for details see Materials and methods). The respective cDNAs were amplified in two rounds of PCR using nested primer sets. This analysis confirmed that A-Mitf is ubiquitous

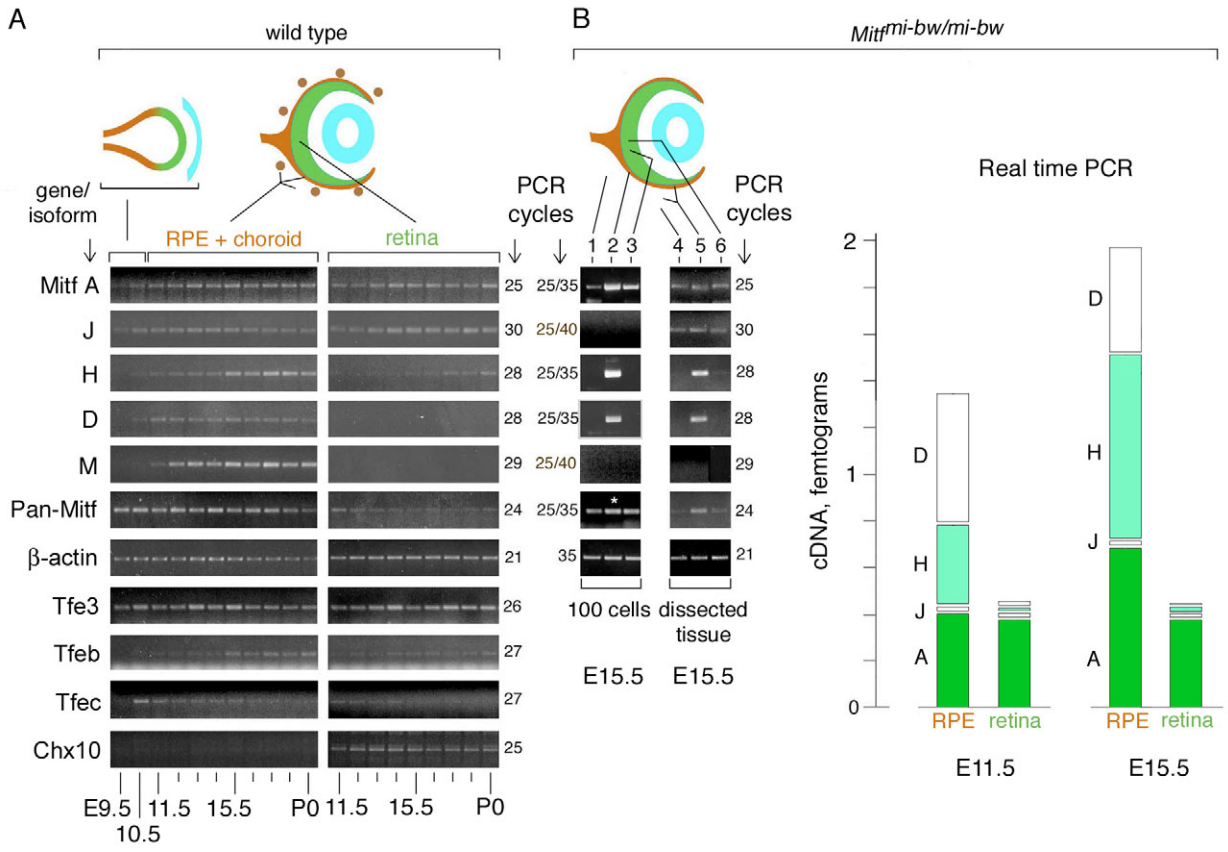

Fig. 3. Differential expression of *Mitf* isoforms during mouse eye development. (**A**) RT-PCR analysis on RNA isolated from wild-type whole optic vesicles (E9.5-10.5) or separate RPE+choroidal and retinal fractions (E11.5-P0). (**B**) RT-PCR (left, lanes 1-6) and real-time PCR (right) for RNA isolated from *Mitf*$^{mi\text{-}bw/mi\text{-}bw}$ eyes, which lack neural crest-derived melanocytes. (Lanes 1-3) E15.5 eyes were dissected as in A and 100 individual cells were microscopically selected as described in Materials and methods. Lane 1, mesenchymal cells; lane 2, RPE cells; lane 3, retinal cells. The asterisk in lane 2 indicates that the corresponding cDNA was diluted 1:10 for the reaction with pan-specific primers. (Lanes 4-6) Pooled fractions from dissected E15.5 eyes as indicated. Lane 4, mesenchymal fraction; lane 5, RPE/mesenchymal fraction; lane 6, retinal fraction. (Right) Real-time PCR. RNA was prepared from separately pooled RPE/mesenchymal and retinal fractions from E11.5 and E15.5 eyes. Results are expressed as mean of absolute amounts of the respective cDNAs and are calculated taking into account that RPE cells represent 7% of the cells in the RPE/mesenchymal fraction. Significance of the difference between RPE and retina (*P*-values, Student's *t*-test; pools of 20 RPE/mesenchymal and retinal fractions each for E11.5, and of 12 RPE/mesenchymal and retinal fractions each for E15.5; four separate assays in triplicate per pool) for E11.5 A-Mitf, >0.1; J-Mitf, <0.1; H-Mitf, <0.001; D-Mitf, <0.00001; and for E15.5 A-Mitf, <0.01; J-Mitf, <0.01; H-Mitf, <0.0001; D-Mitf, <0.001.

and showed that H- and D-Mitf are not only present but in fact enriched in the RPE, compared with retina and mesenchyme. No signals were found for the low-abundance J-Mitf and, as expected, for M-Mitf (Fig. 3B, lanes 1-3). The results are consistent with those obtained from eye tissues dissected using standard techniques (Fig. 3B, lanes 4-6), where A-Mitf and low levels of J-Mitf were found in all fractions (lanes 4-6), H- and D-Mitf were enriched in the fraction that contains RPE and mesenchyme (lane 5), and M-Mitf was absent from all fractions.

The above experiments showed which isoform was expressed in which cell type but did not address the question of their expression levels. In fact, because different primer pairs amplify cDNAs with distinct efficiencies, differences in band intensities cannot be used for comparisons between isoforms. We therefore subjected cDNAs generated from separately pooled RPE/mesenchymal and retinal RNA fractions to real-time PCR using isoform-specific standard curves (see Materials and methods). Fig. 3B (right panel) shows the mean amounts of cDNAs obtained from four repeat assays each for E11.5 and E15.5. Consistent with the results described above, A- and J-Mitf accumulated to similar levels in RPE and retina, and H- and D-Mitf reached higher levels in RPE than in retina. We conclude, therefore, that both the future retina and the future RPE continue to express A- and J-Mitf and that the major isoforms in RPE are D-Mitf and, increasingly with developmental time, H-Mitf.

Genomic deletion of *Mitf* exons 1H, 1D and 1B leads to increased expression of novel mRNA and protein isoforms

To address the question of whether the major RPE isoforms, H- and D-Mitf, are functionally relevant, we analyzed mice homozygous for the *Mitf*$^{mi\text{-}rw}$ (*Mitf red-eyed white*, for short, *rw*) allele which is characterized by a genomic deletion that encompasses the 1H-, 1D- and 1B- exons (Steingrimsson et al., 1994; Hallsson et al., 2000). These mice retain a patch of pigmented coat on the head and occasionally on the belly and have eyes, the sizes of which can vary both between individuals and between the left and right side of the same individual (example shown in Fig. 4A, left side). We first determined the exact boundaries of the deletion and found that it comprises a stretch of 86,346 bp starting downstream of exon 1E and ending upstream of exon 1M (Fig. 4A and see Fig. S1 in the

supplementary material). The deletion has the consequence that the upstream exons, whether coding or not, splice into the next available downstream exon, exon 2A, rather than the normal exon 1B1b (Fig. 4A). Consequently, if translation initiates at the normal start codons in exon 1A, 1C and 1MC, no open reading frames are maintained beyond exon 2 (marked by red dotted lines in Fig. 4A). Novel open reading frames, however, are generated within the normally non-coding exons 1J and 1E (blue lines in Fig. 4A), but the potential AUG start codons do not conform to Kozak rules for efficient translation initiation (Kozak, 1984; Kozak, 1986).

To analyze the transcriptional profile of *Mitf* in eyes of *rw* embryos, we again used RT-PCR as described above, except that whole-eye tissue served as the source of RNA because dissection into RPE/choroid and retina was not feasible with the mutant eyes. Moreover, we used primers covering only the respective single exons to allow for equal product sizes in wild type and *rw*. The results (Fig. 4B) indicate that the expression levels of the upstream exons 1A, 1J and 1E, were increased, whereas those of the downstream exon 1M and the pan-specific exon 9 were decreased. These findings were confirmed by real-time PCR (Fig. 4C). The results showed that at E12.5, for instance, an approximately twofold increase in A-Mitf and a ninefold increase in the minor J-Mitf could not compensate for the lack of the major isoforms, H- and D-Mitf, and for the reduction in M-Mitf that was detectable in these whole-eye extracts (Fig. 4B). At P0, however, isoform-specific increases and decreases cancelled each other out, so that pan-specific amplification of exon 9 gave a *rw*/wild type ratio of ~1.0. Using primers in the specific upstream exons and exon 4, we further confirmed that the overexpressed upstream exons were indeed part of spliced RNAs (Fig. 4D). Note,

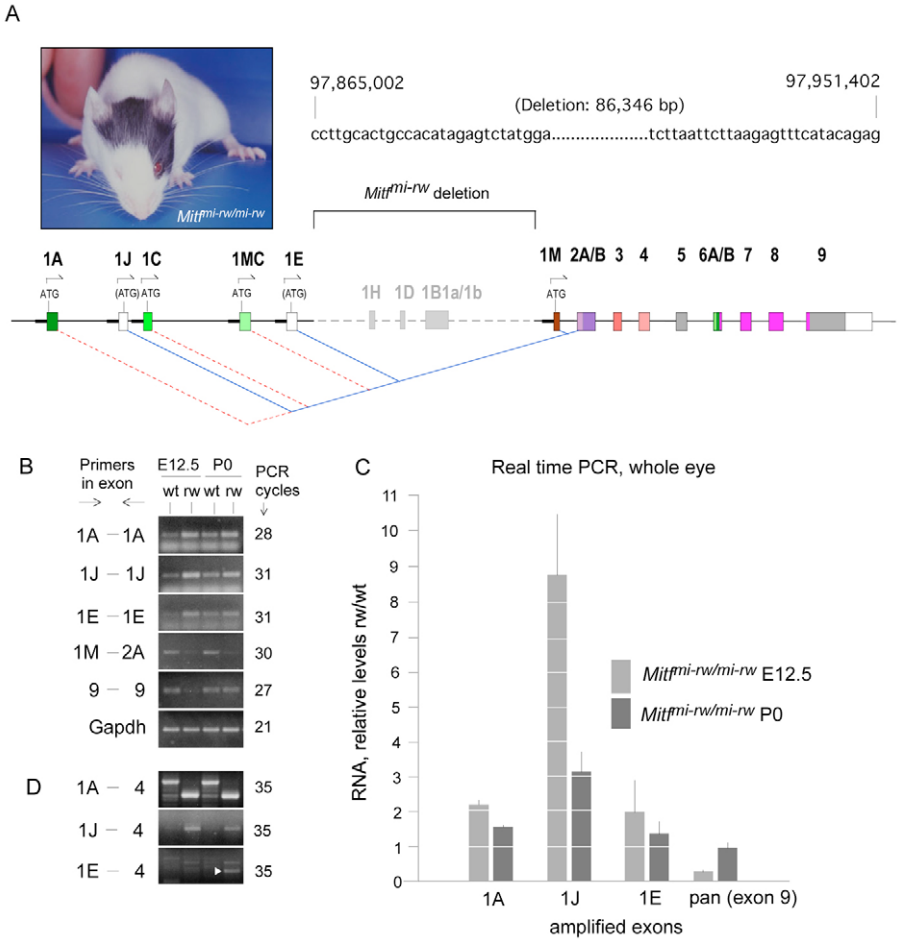

Fig. 4. *Mitf*$^{mi\text{-}rw/mi\text{-}rw}$ mutant mice carry a genomic deletion in *Mitf* encompassing the exons 1H, 1D and 1B. (**A**) Phenotype of an *Mitf*$^{mi\text{-}rw/mi\text{-}rw}$ mutant mouse. Generally, coat pigment patches and eye size are not correlated, as eye size is determined by the development of the RPE and coat patches by neural crest-derived melanocytes. To the right is shown the DNA sequence flanking the genomic deletion, with the numbers of the first and last base referring to the positions on chromosome 6 according to assembly NCBIM36. The schematic beneath shows the extent of the deletion and highlights the novel splice junctions that are generated between the upstream exons 1A, 1J, 1C, 1MC and 1E and the downstream exon 2A. For details, see text. (**B**) RT-PCR using RNA from E12.5 wild-type and *Mitf*$^{mi\text{-}rw}$ (*rw*) mutant embryos and the corresponding P0 newborns. Note increased band intensity in *rw* with exons 1A, 1J and 1E, but decreased band intensity at E12.5 with pan-specific primers (exon 9). (**C**) Real-time PCR from RNA of whole eyes harvested at the indicated ages, using primers as in B. The results are expressed as RNA levels in *rw* mutants relative to those in corresponding wild-type embryos (groups of 14 eyes each, three measurements each in triplicate). The increases in *rw* over wild type in 1A and 1J, as well as the decrease in exon 9 at E12.5, are statistically significant ($P<0.01$, Student's *t*-test). *P*-values for the increase in 1E are <0.02 at E12.5 and =0.13 at P0. No significant difference was found for exon 9 at P0 ($P=0.27$). (**D**) RT-PCR using primers spanning four exons. Note the differently sized products in wild type and *rw* for isoform 1A. For isoform 1J, the expected larger product in wild type is not seen because its relative level is low (see Fig. 2), but the smaller sized product in *rw* is visible. In 1E-4, the white arrowhead points to the correct E-Mitf band.

however, that even though the exon 1E-specific forward and reverse primers gave a visible band in wild type (Fig. 4B), no correctly sized band was seen in wild type with primers in exons 1E and 4 (Fig. 4D). This confirms the finding mentioned above that spliced transcripts containing exon 1E are below the detection threshold in the developing eye.

The lack of normal open reading frames in the internally deleted mRNAs suggested that *Mitf*$^{mi\text{-}rw}$ is a functional null allele. Intriguingly, however, when we tested corresponding expression constructs in transfection or in vitro transcription/translation assays, we found that MITF proteins were generated that reacted with the antibody to the MITF C-terminal domain. Further analyses showed that the translation of these proteins is initiated predominantly from an internal AUG codon corresponding to Met62 in exon 2B, and that the N-terminally truncated proteins accumulate in the cell nucleus and are transcriptionally active on target gene promoters, including the promoter of the melanin biosynthetic enzyme gene tyrosinase (see Fig. S2 in the supplementary material). These results suggest that *rw* mice might retain *Mitf* activity associated with the novel protein isoforms despite the lack of H- and D-Mitf.

Deletion of *Mitf* exons 1H, 1D and 1B interferes with normal eye development but allows for partial pigmentation

To determine the in vivo consequence of the *rw* deletion, we analyzed the development of *rw* eyes in detail. As shown in Fig. 5, in situ hybridization with a pan-*Mitf*-specific probe indicated that *Mitf* mRNAs are indeed expressed at the expected locations in the developing *rw* eyes. At E12.5, however, their levels were reduced compared with wild type, but at E17.5, they were close to normal (Fig. 5, compare A with B, E with F). Immunohistochemistry using pan-specific antibodies indicated a reduced signal in *rw* at both ages, which is likely to reflect a reduced translational efficiency of the *rw* mRNAs compared with wild-type RNAs (Fig. 5, compare C with D, G with H). Despite the low MITF protein levels, however, a clear signal for tyrosinase was found in *rw* RPE, particularly at E17.5 (Fig. 5I-L), in contrast to developing eyes from *Mitf*-null mutants, which lack tyrosinase expression (Nakayama et al., 1998). Consistent with this result, pigmentation, although at low levels, could be found in the *rw* peripheral RPE and iris (Fig. 5M,N) as well as in the neuroepithelial part of the adult iris (Fig. 5O,P). Nevertheless, RPE development was perturbed, either because the overall MITF protein levels were too low or because full-length proteins containing the normal N-terminal sequences were missing. Much as in developing eyes of other *Mitf* mutants (Müller, 1950; Bumsted and Barnstable, 2000; Nguyen and Arnheiter, 2000), the dorsal RPE became thick (Fig. 5Q,R), retained high-level PAX6 expression (Fig. 5Q-T), and eventually transdifferentiated into a laminated second retina (not shown). In some eyes, however, the RPE abnormalities were characterized not by a general thickening but by foldings (Fig. 5S,T), a much milder abnormality than seen in other *rw* eyes. The results suggest that the lack of H- and D-MITF and exon 1B leads to RPE abnormalities of variable severity, but that the novel MITF protein isoforms are still capable of inducing pigmentation of the ciliary margin and the iris.

Lack of CHX10, a negative regulator of *Mitf*, leads to an increase in H- and D-Mitf in the retina

The downregulation of *Mitf* during retinal development involves a pathway that is initiated by extracellular signals emanating from the surface ectoderm, notably FGF1/2, and includes the paired-like homeodomain transcription factor CHX10 that negatively regulates *Mitf* expression in the retina (schematically indicated in Fig. 6A). As previously shown in *Chx10*$^{orJ/orJ}$ (*Chx10-ocular retardation*) mutant embryos, which lack functional copies of *Chx10*, the future retina is hypoplastic (Konyukhov and Sazhina, 1966; Burmeister et al., 1996; Green et al., 2003) and *Mitf* mRNA and protein levels are increased

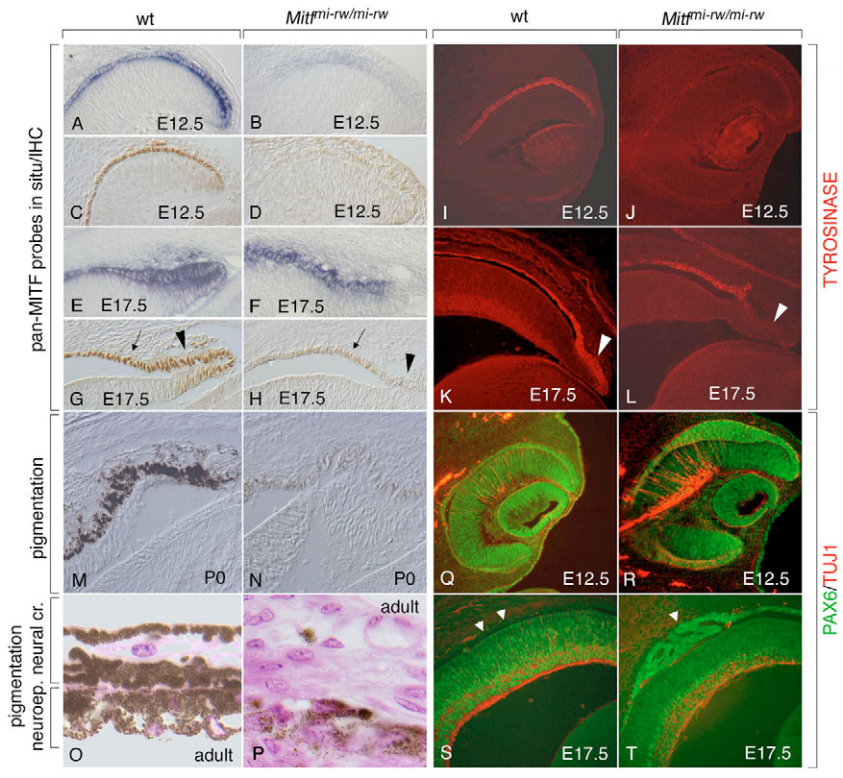

Fig. 5. The *Mitf*$^{mi\text{-}rw}$ allele allows for the expression of *Mitf* and its target gene tyrosinase in the anterior RPE as well as for residual pigmentation in the iris but leads to an abnormal RPE dorsally. Sections of wild-type (wt) and *Mitf*$^{mi\text{-}rw/mi\text{-}rw}$ mutant mouse eyes of the indicated ages were stained with a pan-Mitf in situ probe (**A**,**B**,**E**,**F**), a pan-MITF antiserum (**C**,**D**,**G**,**H**), antibodies against tyrosinase (**I-L**), or against PAX6 (green) and TUJ1 (red) (**Q-T**). Note that the mutant eye expresses *Mitf* RNA (B,F) and low levels of MITF protein, along with tyrosinase, particularly at later stages (compare G with H, arrows; K with L). Also note that in the mutant at E17.5, the distal ciliary margin, although positive for *Mitf* RNA (F), is relatively free of MITF and tyrosinase (arrowhead in H and L, compare with arrowhead in G and K). (**M**,**N**) Strong pigmentation at P0 in wild type (M) and weak pigmentation in *rw* (N). (**O**,**P**) Pigmentation in adult wild-type iris (O) and *rw* iris (P). (Q,R) Dorsal thickening of the E12.5 RPE in *rw* (R) compared with wild type (Q). (S,T) RPE abnormalities in *rw* at E17.5. Arrowheads in S mark the location of the wild-type RPE, which now is free of PAX6 staining. By contrast, mutant RPE retains PAX6 staining and in this eye showed epihelial folds rather than homogeneous thickening (arrowhead in T).

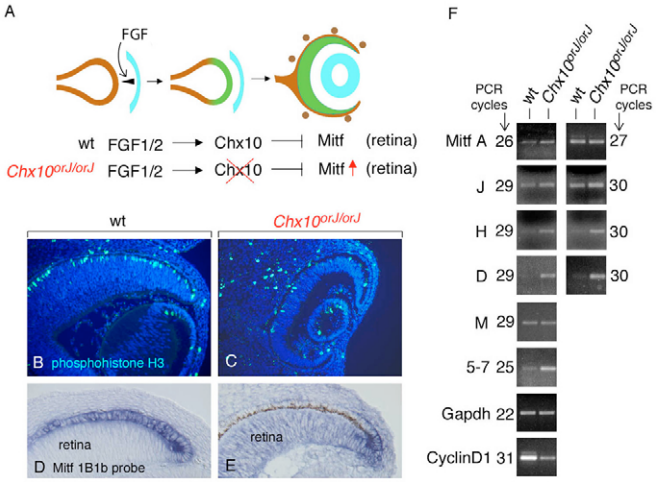

Fig. 6. Lack of downregulation of *Mitf* in *Chx10*$^{orJ/orJ}$ retinas predominantly affects H- and D-Mitf. (**A**) Genetic pathway showing the downregulation of *Mitf* in the future retina by FGFs emanating from the surface ectoderm (light blue) and *Chx10* operating in the distal optic neurepithelium. In *Chx10* mutant mice, *Mitf* is not downregulated in the future retina and the retina hypoproliferates. (**B-E**) Cryostat sections from E13.5 wild-type (wt) (B,D) and *Chx10*$^{orJ/orJ}$ (C,E) eyes labeled for phosphohistone H3 (B,C) or by in situ hybridization using an *Mitf* exon 1B1b probe (D,E). Note upregulation of exon-1B1b-containing RNA in mutant (E) compared with wild-type (D) retina. Also note that the section in E comes from an embryo with a pigmented RPE (brown stain), whereas the one in D comes from an albino embryo. (**F**) Limited-cycle RT-PCR analysis performed on RNA isolated from wild-type and *Chx10*$^{orJ/orJ}$ whole eyes at E13.5. Primers for A-, J-, H-, D- and M-Mitf are as used for Fig. 3A. For pan-specific amplification, primers in exon 5 and 7 were used. Note that for A- and J-Mitf, at the lower number of PCR cycles the intensities of the bands are slightly increased in mutant compared with wild-type eyes, but at the higher number of cycles the difference is no longer visible. No such differences are seen for M-Mitf. H- and D-Mitf, however, show a clear difference between wild type and mutant at both 29 and 30 cycles of amplification. The use of primers specific for cyclin D1 indicates a reduction in mutant, consistent with the corresponding retinal hypoproliferation.

(Rowan et al., 2004; Horsford et al., 2005). To confirm that the mutant retina hypoproliferates, we used phosphohistone H3 labeling to mark the cells at the G2–M transition. As expected, the thinner *Chx10*$^{or\text{-}J/or\text{-}J}$ retina showed substantially fewer labeled cells (Fig. 6B,C). As shown in Fig. 6D,E, this phenotype is correlated with the retinal retention of *Mitf* RNAs containing exon 1B1b. To dissect the isoform composition of the upregulated RNA, we used limiting cycle RT-PCR of RNA extracted from wild-type and *Chx10* mutant eyes at E13.5. The results (Fig. 6F) revealed a substantial increase in H- and D-Mitf, but a barely perceptible increase in A- and J-Mitf. Theoretically, a specific retinal upregulation of A- and J-Mitf might have been partially masked by the ubiquitous expression of these isoforms outside the retina. This is unlikely, though, because retinal changes in the expression of cyclin D1, which is also expressed outside the retina, could easily be detected in the whole-eye extracts, and A- and J-Mitf continued to be expressed throughout development in the *Chx10*-positive wild-type retina (see Fig. 2).

To determine whether CHX10 interacts in vivo with *Mitf* promoters, we performed chromatin immunoprecipitation (ChIP) assays using extracts of eye primordia at E10.5-11.0, corresponding to the period during which *Mitf* is downregulated in the retina. The results indicate a weak interaction of CHX10 with a binding site in the A-Mitf promoter, and strong interactions with a site in the H-Mitf promoter and with at least two sites in the D-Mitf promoter (see Figs S3, S4 in the supplementary material). Taken together, the results suggest that H- and D-Mitf are the major, and likely direct, targets of the *Chx10*-mediated *Mitf* downregulation in the retina, whereas A- and J-Mitf are not much affected by *Chx10*.

Deletion of *Mitf* exons 1H, 1D and 1B corrects the retinal hypoproliferation phenotype in *Chx10* mutant embryos

The above results prompted us to determine whether the lack of H- and D-MITF and exon 1B, as seen in *rw* embryos, might be sufficient to correct the *Chx10*-mediated retinal hypoproliferation phenotype. Such a correction has thus far only been described with dominant-negative *Mitf* mutations that equally affect all isoforms (Konyukhov and Sazhina, 1966; Horsford et al., 2005; Bharti et al., 2006). Therefore, we intercrossed *Chx10*$^{orJ/orJ}$ mice with *Mitf*$^{mi\text{-}rw/mi\text{-}rw}$ mice to generate double homozygotes. Staining for cyclin D1 in conjunction with PAX6 and the neuronal marker TUJ1 [β-3-tubulin (TUBB3)] indicated that, as expected, eyes from *Mitf*$^{mi\text{-}rw}$ newborns (Fig. 7A,E,I) had a retinal thickness and lamination similar to those of wild type (Fig. 7D,H,L), whereas eyes from *Chx10*^{orJ} newborns showed the severe retinal hypoproliferation and retina-to-RPE transdifferentiation described previously (Burmeister et al., 1996; Rowan et al., 2004; Horsford et al., 2005) (Fig. 7B,F,J). In the double *Mitf*$^{mi\text{-}rw}$;*Chx10*^{orJ} homozygotes, however, cyclin D1 staining and retinal thickness were nearly normal, although retinal lamination was still abnormal (Fig. 7C,G,K). This result indicates that in *Chx10* mutants, *Mitf* upregulation, once deprived of the contribution of H- and D-Mitf and exon 1B, no longer leads to retinal hypoproliferation. This is consistent with earlier observations showing that dominant-negative *Mitf* mutations partially correct the *Chx10* mutant phenotype (Konyukhov and Sazhina, 1966; Horsford et al., 2005).

DISCUSSION

The dissection of the expression patterns of *Mitf* isoforms has shown that some isoforms, such as H- and D-Mitf, are present in a temporally and spatially restricted manner whereas others, such as A- and J-Mitf, are found ubiquitously both within and outside the optic neuroepithelium. The notion that H- and D-Mitf are more important for eye development than other isoforms rests on several lines of reasoning. First, H- and D- Mitf consistently accumulate to higher levels in the RPE than other isoforms. Second, retinal hypoproliferation in *Chx10* mutants is associated with abnormally high levels of H- and D-Mitf, but not of A- and J-Mitf or other isoforms. Third, the lack of H- and D-Mitf in *Mitf red-eyed white* mutants, although confounded by complex changes in mRNAs and protein isoforms, is clearly associated with developmental eye defects. Fourth, when H- and D-Mitf are missing in *Chx10* mutants, retinal development is restored. It appears, therefore, that H- and D-Mitf need to be precisely regulated during eye development, whereas the absence of other isoforms, or their presence in the retina, is more readily tolerated.

The fact that upstream *Mitf* regulatory regions contain distinct transcription-factor-binding motifs that are conserved across mammalian and avian species (Hallsson et al., 2007) argues strongly for a transcriptional control of the different *Mitf* isoforms. For instance, the ubiquitously active A-Mitf promoter has potential binding sites for transcription factors with widespread expression patterns such as MYC/MAX, STAT and SP1 (Hallsson et al., 2007).

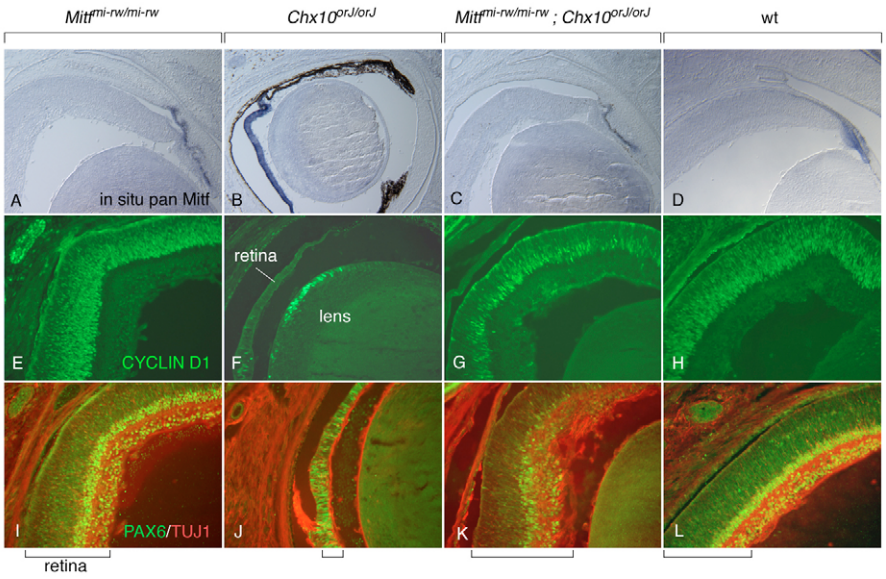

Fig. 7. The *Mitf*$^{mi\text{-}rw}$ allele partially rescues the *Chx10*^{orJ} mutant phenotype. Eyes from newborn mice of the indicated genotypes were sectioned and processed for in situ hybridization with a pan-*Mitf* probe (**A-D**), cyclin D1 immunofluorescence (**E-H**), or PAX6/TUJ1 double immunofluorescence (**I-L**). Compared with wild-type (wt), *Mitf*$^{mi\text{-}rw/mi\text{-}rw}$ retinas appear normal, both in thickness and in staining. By contrast, *Chx10*$^{orJ/orJ}$ retinas retain *Mitf* expression and are severly hypoplastic, with a pigmented monolayer replacing the retina particularly in the distal part (B). Moreover, they show fewer cyclin D1-positive and PAX6-positive cells (F,J). Eyes from *Mitf*$^{mi\text{-}rw/mi\text{-}rw}$;*Chx10*$^{orJ/orJ}$ double mutants, however, have retinas of relatively normal appearance and thickness even though their PAX6 staining and lamination are still abnormal (C,G,K). Brackets at the bottom mark the thickness of the retina.

By contrast, the H- and D-Mitf promoters have potential binding sites for the retina-specific transcription factor CHX10 (Hallsson et al., 2007) (this paper), precisely the factor involved in the retinal downregulation of these two promoters. In fact, ChIP assays clearly indicate that at least some of these sites are occupied by CHX10 in vivo, suggesting a direct regulation of the respective *Mitf* promoters by this transcription factor.

A separate control of each promoter does not however exclude the presence of additional mechanisms by which distinct *Mitf* mRNAs are co-regulated. A transcriptional co-regulatory mechanism has been suggested by the observation, made by immunofluorescence, that *Pax2*/*Pax6* double knock-out mice lack MITF protein expression in the optic neuroepithelium and that the human A-MITF promoter contains binding sites for PAX2/PAX6, suggesting that it acts as a control region for all ocular *MITF* expression (Bäumer et al., 2003). These binding sites, however, are not well conserved across mammalian and avian species. Hence, it is possible that even in *Pax2*/*Pax6* double knock-out mice, the ubiquitously expressed A- and J-MITF, which are undetectable by immunofluorescence on histological sections (data not shown), might continue to be present, and only the major and immunofluorescently detectable H- and D-MITF are absent. A different, post-transcriptional co-regulatory mechanism is suggested by the conservation, in the 3′UTR, of potential recognition sites for microRNAs, some of which are thought to be controlled by *Chx10* (Hallsson et al., 2007; Xu et al., 2007). In fact, microRNAs are excellent candidates to contribute to the retinal downregulation of all *Mitf* mRNAs that share the same 3′UTR, but the contribution of these microRNAs is likely to be small and might not exceed the minor effects that *Chx10* has, for instance, on the levels of A- and J-Mitf.

The fact that each of the nine promoters is linked to a unique exon also leads to the important question of whether multiple promoters exist solely to provide the correct levels of MITF protein at each developmental time point and location, or whether they exist to generate mRNAs or proteins with isoform-specific functions. Indeed, some evidence suggests that sequence differences at the MITF N-terminus can influence the proteins' activities. For instance, ectopic expression of ascidian *Mitf*, the N-terminal sequence of which resembles A-MITF, induces additional pigment cells in ascidian larvae, as does mouse A-MITF, but not mouse H- or M-MITF (Yajima et al., 2003). Furthermore, A-, MC- and E-MITF regulate distinct sets of target genes in *Mitf*-null mutant mast cells (Shahlaee et al., 2007). There is also evidence, however, that expression levels are more important than specific sequences in determining MITF activities. For instance, regardless of whether A-MITF or M-MITF was expressed in quail neuroepithelial cells, pigmented colonies arose that consisted of RPE-like epithelial cells, in which MITF was low, and of neural crest-like dendritic cells, in which MITF was high (Planque et al., 2004). Our findings with the natural *Mitf*$^{mi\text{-}rw}$ deletion suggest, in fact, that low levels of N-terminally truncated MITF proteins are capable of inducing pigmentation in the ciliary margin and the neuroepithelial portions of the iris, whereas in the complete absence of *Mitf* no such pigmentation is ever seen (Hodgkinson et al., 1998; Nakayama et al., 1998). This finding is consistent with the fact that N-terminally truncated MITFs retain activity on promoters of pigmentation genes, including the promoter of tyrosinase, which encodes the rate-limiting enzyme for melanin synthesis (see Fig. S2 in the supplementary material). On the other hand, the dorsal RPE is still abnormal in *Mitf*$^{mi\text{-}rw}$ embryos. It is conceivable, therefore, that full RPE development, in contrast to mere pigmentation, depends on the presence of the upstream coding exons, perhaps on exon 1B1b in particular. This exon contains a glutamine-rich domain, thought to be involved in protein-protein interactions, that is conserved in vertebrates and flies (Hallsson et al., 2007) and is reminiscent of similar domains in other transcription factors such as CREB and SP1. That cell differentiation does not require this domain, however, is evident from the fact that M-MITF is sufficient to induce pigmentation upon experimental expression in cultured cells (Bejar et al., 2003), and that *Mitf*$^{mi\text{-}rw}$ mice show RPE and iris pigmentation as well as some pigmented spots in the coat. In any event, a definitive answer to the question of why there are distinct promoters must await results from targeted promoter/exon knockouts and isoform-specific rescue experiments.

In addition to highlighting the importance of alternative promoter use, our study of the *Mitf*$^{mi\text{-}rw}$ deletion also draws attention to alternative translation initiation. Alternative translation start sites have been observed in several genes and, much as with alternative promoter use, can contribute to functional diversity in wild type and alter disease in mutants (Sandelin et al., 2007; Scheper et al., 2007; Zhang et al., 2007). The fact that in the *rw* mutant mice, translation can be initiated from downstream start codons, suggests that these

codons might be utilized for initiation even in the context of a wild-type sequence, although at low efficiency. Whether this is biologically relevant, however, remains to be explored.

Finally, the fact that the *Mitf*$^{mi\text{-}rw}$ deletion is associated with random bilateral asymmetries in eye development merits special consideration. The fact that genetically identical cells, even if exposed to the same environment, can show substantial variations in phenotypic manifestations is thought to result from 'stochastic' variations in gene expression that are likely to be due to variant epigenetic chromatin states (for a review, see Kaern et al., 2005). It is reasonable to assume that high levels of gene expression will generally buffer cells against random fluctuations in their molecular composition and so ensure a normal embryonic development. If, however, only threshold levels of gene expression are achieved, as is the case for *Mitf* in *rw* mice with their abnormal *Mitf* transcripts, stochastic fluctuations in epigenetic states might lead to major phenotypic differences between individual cells. Given that epigenetic states can be passed on through cell divisions, cellular variations might lead to tissue variations and so to differences between organs that are normally bilaterally symmetrical. Hence, our study of *Mitf* isoforms not only touches on the complexities by which a single gene controls organogenesis, but also on the intriguing question of how bilateral symmetries are being generated and maintained.

We thank Dr Vincent Hearing for antibodies to tyrosinase, the NINDS Sequencing Facility and the Animal Health and Care Section for excellent services, and Drs Dubois-Dalcq and Brian Howell and the members of the Mammalian Development Section for helpful comments on the manuscript. This work was supported in part by grants from the Italian Telethon Foundation to S.B. and by the Intramural Research Program of the NIH, NINDS.

Supplementary material

Supplementary material for this article is available at http://dev.biologists.org/cgi/content/full/135/6/1169/DC1

References

Amae, S., Fuse, N., Yasumoto, K., Sato, S., Yajima, I., Yamamoto, H., Udono, T., Durlu, Y. K., Tamai, M., Takahashi, K. et al. (1998). Identification of a novel isoform of microphthalmia-associated transcription factor that is enriched in retinal pigment epithelium. *Biochem. Biophys. Res. Commun.* **247**, 710-715.

Arnheiter, H., Hou, L., Nguyen, M. T. T., Bismuth, K., Csermely, T., Murakami, H., Skuntz, S., Liu, W. and Bharti, K. (2006). Mitf – a matter of life and death for the developing melanocyte. In *From Melanocytes to Melanoma: The progression to Malignancy* (ed. V. Hearing and S. P. L. Leong), pp. 27-49. Totowa, NJ: Humana Press.

Bäumer, N., Marquardt, T., Stoykova, A., Spieler, D., Treichel, D., Ashery-Padan, R. and Gruss, P. (2003). Retinal pigmented epithelium determination requires the redundant activities of Pax2 and Pax6. *Development* **130**, 2903-2915.

Bejar, J., Hong, Y. and Schartl, M. (2003). Mitf expression is sufficient to direct differentiation of medaka blastula derived stem cells to melanocytes. *Development* **130**, 6545-6553.

Bharti, K., Nguyen, M. T., Skuntz, S., Bertuzzi, S. and Arnheiter, H. (2006). The other pigment cell: specification and development of the pigmented epithelium of the vertebrate eye. *Pigment Cell Res.* **19**, 380-394.

Bora, N., Conway, S. J., Liang, H. and Smith, S. B. (1998). Transient overexpression of the Microphthalmia gene in the eyes of Microphthalmia vitiligo mutant mice. *Dev. Dyn.* **213**, 283-292.

Bumsted, K. M. and Barnstable, C. J. (2000). Dorsal retinal pigment epithelium differentiates as neural retina in the microphthalmia (mi/mi) mouse. *Invest. Ophthalmol. Vis. Sci.* **41**, 903-908.

Burmeister, M., Novak, J., Liang, M. Y., Basu, S., Ploder, L., Hawes, N. L., Vidgen, D., Hoover, F., Goldman, D., Kalnins, V. I. et al. (1996). Ocular retardation mouse caused by Chx10 homeobox null allele: impaired retinal progenitor proliferation and bipolar cell differentiation. *Nat. Genet.* **12**, 376-384.

Carninci, P., Sandelin, A., Lenhard, B., Katayama, S., Shimokawa, K., Ponjavic, J., Semple, C. A., Taylor, M. S., Engstrom, P. G., Frith, M. C. et al. (2006). Genome-wide analysis of mammalian promoter architecture and evolution. *Nat. Genet.* **38**, 626-635.

Green, E. S., Stubbs, J. L. and Levine, E. M. (2003). Genetic rescue of cell number in a mouse model of microphthalmia: interactions between Chx10 and G1-phase cell cycle regulators. *Development* **130**, 539-552.

Hallsson, J. H., Favor, J., Hodgkinson, C., Glaser, T., Lamoreux, M. L., Magnusdottir, R., Gunnarsson, G. J., Sweet, H. O., Copeland, N. G., Jenkins, N. A. et al. (2000). Genomic, transcriptional and mutational analysis of the mouse microphthalmia locus. *Genetics* **155**, 291-300.

Hallsson, J. H., Haflidadottir, B. S., Schepsky, A., Arnheiter, H. and Steingrimsson, E. (2007). Evolutionary sequence comparison of the Mitf gene reveals novel conserved domains. *Pigment Cell Res.* **20**, 185-200.

Hershey, C. L. and Fisher, D. E. (2005). Genomic analysis of the Microphthalmia locus and identification of the MITF-J/Mitf-J isoform. *Gene* **347**, 73-82.

Hodgkinson, C. A., Moore, K. J., Nakayama, A., Steingrimsson, E., Copeland, N. G., Jenkins, N. A. and Arnheiter, H. (1993). Mutations at the mouse microphthalmia locus are associated with defects in a gene encoding a novel basic-helix-loop-helix-zipper protein. *Cell* **74**, 395-404.

Hodgkinson, C. A., Nakayama, A., Li, H., Swenson, L. B., Opdecamp, K., Asher, J. H., Jr, Arnheiter, H. and Glaser, T. (1998). Mutation at the anophthalmic white locus in Syrian hamsters: haploinsufficiency in the Mitf gene mimics human Waardenburg syndrome type 2. *Hum. Mol. Genet.* **7**, 703-708.

Horsford, D. J., Nguyen, M. T., Sellar, G. C., Kothary, R., Arnheiter, H. and McInnes, R. R. (2005). Chx10 repression of Mitf is required for the maintenance of mammalian neuroretinal identity. *Development* **132**, 177-187.

Kaern, M., Elston, T. C., Blake, W. J. and Collins, J. J. (2005). Stochasticity in gene expression: from theories to phenotypes. *Nat. Rev. Genet.* **6**, 451-464.

Konyukhov, B. V. and Sazhina, M. V. (1966). Interaction of the genes of ocular retardation and microphthalmia in mice. *Folia Biol. Praha* **12**, 116-123.

Kozak, M. (1984). Point mutations close to the AUG initiator codon affect the efficiency of translation of rat preproinsulin in vivo. *Nature* **308**, 241-246.

Kozak, M. (1986). Point mutations define a sequence flanking the AUG initiator codon that modulates translation by eukaryotic ribosomes. *Cell* **44**, 283-292.

Liu, I. S., Chen, J. D., Ploder, L., Vidgen, D., van der Kooy, D., Kalnins, V. I. and McInnes, R. R. (1994). Developmental expression of a novel murine homeobox gene (Chx10): evidence for roles in determination of the neuroretina and inner nuclear layer. *Neuron* **13**, 377-393.

Müller, G. (1950). Eine entwicklungsgeschichtliche Untersuchung über das erbliche Kolobom mit Mikrophthalmus bei der Hausmaus. *Z. Mikrosk. Anat. Forsch.* **56**, 520-558.

Nakayama, A., Nguyen, M. T., Chen, C. C., Opdecamp, K., Hodgkinson, C. A. and Arnheiter, H. (1998). Mutations in microphthalmia, the mouse homolog of the human deafness gene MITF, affect neuroepithelial and neural crest-derived melanocytes differently. *Mech. Dev.* **70**, 155-166.

Nguyen, M. and Arnheiter, H. (2000). Signaling and transcriptional regulation in early mammalian eye development: a link between FGF and MITF. *Development* **127**, 3581-3591.

Planque, N., Raposo, G., Leconte, L., Anezo, O., Martin, P. and Saule, S. (2004). Microphthalmia transcription factor induces both retinal pigmented epithelium and neural crest melanocytes from neuroretina cells. *J. Biol. Chem.* **279**, 41911-41917.

Rowan, S., Chen, C. M., Young, T. L., Fisher, D. E. and Cepko, C. L. (2004). Transdifferentiation of the retina into pigmented cells in ocular retardation mice defines a new function of the homeodomain gene Chx10. *Development* **131**, 5139-5152.

Sandelin, A., Carninci, P., Lenhard, B., Ponjavic, J., Hayashizaki, Y. and Hume, D. A. (2007). Mammalian RNA polymerase II core promoters: insights from genome-wide studies. *Nat. Rev. Genet.* **8**, 424-436.

Scheper, G. C., van der Knaap, M. S. and Proud, C. G. (2007). Translation matters: protein synthesis defects in inherited disease. *Nat. Rev. Genet.* **8**, 711-723.

Shahlaee, A. H., Brandal, S., Lee, Y. N., Jie, C. and Takemoto, C. M. (2007). Distinct and shared transcriptomes are regulated by microphthalmia-associated transcription factor isoforms in mast cells. *J. Immunol.* **178**, 378-388.

Steingrimsson, E., Moore, K. J., Lamoreux, M. L., Ferre-D'Amare, A. R., Burley, S. K., Zimring, D. C., Skow, L. C., Hodgkinson, C. A., Arnheiter, H., Copeland, N. G. et al. (1994). Molecular basis of mouse microphthalmia (mi) mutations helps explain their developmental and phenotypic consequences. *Nat. Genet.* **8**, 256-263.

Steingrimsson, E., Copeland, N. G. and Jenkins, N. A. (2004). Melanocytes and the microphthalmia transcription factor network. *Annu. Rev. Genet.* **38**, 365-411.

Xu, S., Witmer, P. D., Lumayag, S., Kovacs, B. and Valle, D. (2007). MicroRNA transcriptome of mouse retina and identification of a sensory organ specific miRNA cluster. *J. Biol. Chem.* **282**, 25053-25066.

Yajima, I., Sato, S., Kimura, T., Yasumoto, K., Shibahara, S., Goding, C. R. and Yamamoto, H. (1999). An L1 element intronic insertion in the black-eyed white (Mitf[mi-bw]) gene: the loss of a single Mitf isoform responsible for the pigmentary defect and inner ear deafness. *Hum. Mol. Genet.* **8**, 1431-1441.

Yajima, I., Endo, K., Sato, S., Toyoda, R., Wada, H., Shibahara, S., Numakunai, T., Ikeo, K., Gojobori, T., Goding, C. R. et al. (2003). Cloning and functional analysis of ascidian Mitf in vivo: insights into the origin of vertebrate pigment cells. *Mech. Dev.* **120**, 1489-1504.

Zhang, J., Cai, J. and Li, Y. (2007). A genome-wide survey of alternative translational initiation events in Homo sapiens. *Sci. China C Life Sci.* **50**, 423-428.